Peer-reviewed version available at *Water* **2018**, *10*, 745; doi:10.3390/w10060745

Article

Uptake Fluoride from Water by Starch Stabilized Layered Double Hydroxide

Jiming Liu[1], Xiuping Yue[1,*], Xinyu Lu[1], Yu Guo[1]

[1] College of Environment Science and Engineering, Taiyuan University of Technology, Shanxi, China ; liujiming@tyut.edu.cn(J.L.); luxinyu@tyut.edu.cn(X.L.); 676618568@qq.com(Y.G.)

* Correspondence: yuexiuping@tyut.edu.cn; Tel.: +86 351 6010243

Abstract: A novel starch stabilized Mg/Al LDHs material (S-LDH) was prepared in a facile approach and its fluoride ion removal performance was developed. Characterization of S-LDH was employed by using XRD, FTIR and particle size distribution. The adsorption property was studied through the assessment of adsorption isotherms, kinetic models, thermal dynamics and pH influence. The result shows that a low loading of starch of 10 mg onto LDH could obviously improve fluoride removal rate. The S-LDH had 3 times higher adsorption capacity to fluoride than that of Mg/Al LDH to fluoride. The particle size was smaller and the particle size distribution was narrower for S-LDH than that for Mg/Al LDH. Langmuir adsorption isotherm model and pseudo-second-order kinetic model fitted well with the experimental data. In thermodynamic parameters, the enthalpy (ΔH^0) value was 35.63 kJ mol^{-1} and the entropy (ΔS^0) value was 0.0806 kJ $mol^{-1}K^{-1}$. The values of ΔG^0 were negative, implying the adsorption process is spontaneous. S-LDH reveals stable adsorption property in a wide pH range from 3 to 9. The mechanism for fluoride adsorption on S-LDH included surface adsorption and interaction ion exchange.

Keywords: Layered double hydroxides; Hydrotalcite; Starch; Fluoride; Adsorption property; Thermodynamics

1. Introduction

Many reports indicate high fluoride content exist in drinking water in many countries like China, Russia, Pakistan, South Africa[1-3]. Use of drinking water containing high concentration of fluoride can cuse dental fluorosis, nervous system diseases, and even cancer[4-6]. The world health organization (WHO) has set the guideline on fluoride in drinking water at 1.5 mg/L[7]. Plenty of methods have been attempted to low down high level fluoride, including electrodialysis[8],adsorption[9-12], precipitation[13], ion exchange[14] and membrane filteration[15]. Among them, adsorption is found to be more appropriate method to remove fluoride in drinking water due to the fact that it is relatively simple in design and convenient to operate.

In recent years, Layered double hydroxides (LDHs) have attracted increasing attention in catalysis, adsorption, ion exchange, etc. and have been regarded as effective adsorbent in reducing the contents of excessive anions, including fluoride[12, 16-18]. LDHs are composed of alternating stacked cationic layers and interlayer compensation anions. The basic structural formula is: $M^{2+}_{1-x}M^{3+}_{x}(OH)_2(A^{n-})_{x/n}\cdot mH_2O$, wherein M^{2+} and M^{3+} represent divalent and trivalent cations, respectively, and A^{n-} represents an n-valent anion. Typical LDHs are $Mg_6Al_2(OH)_{16}CO_3^{2-}\cdot 4H_2O$, which have a structure similar to brucite $Mg(OH)_2$, and consist of Mg^{2+} and Al^{3+} ions on both sides, with CO_3^{2-} anion and water molecules in that middle, like sandwich bread. LDHs own a large interlayer surface, which can capture all kinds of different exchangeable anionic species, provide it high removal efficiency of anionic compounds. However, investigation shows that carbonate anion(CO_3^{2-}) is easily generated by CO_2 in the air, enters the intermediate layer and its strong affinity prevents the substitution of other anions unless it is further calcined, thus leading to LDHs which cannot be regarded as exchangeable inorganic anionic materials[19]. It has been reported that remove rate of fluoride ions by Mg/Al LDHs is only 29.8%[20].

To overcome these drawbacks, a kind of corn starch was applied to the preparation of synthesizing starch-stabilized LDHs, and its usage in fluoride removal was examined. The starch-stabilized nanoparticles have many merits and received worldwide attention because of their good biodegradability, environmentally

friendly, and low cost[21]. The starch-based materials exhibited much less agglomeration and greater reactivity than those without starch, thereby accelerating the physical property of the compounds. Liang, q, q studied the removal of $A_SO_4^{2-}$ by starch stabilized magnetite and the results showed that the adsorption capacity of stabilized magnetite is 14% higher than that of original magnetite[22]. Therefore, In this present work, a novel starch stabilized Mg/Al LDHs material (S-LDH) was developed to study its fluoride ion removal performance. Characterization of S-LDH was employed by using XRD, FTIR and particle size distribution. The adsorption mechanism was studied through the assessment of adsorption isotherms, kinetic models, thermal dynamics and pH influence.

2. Materials and Methods

2.1. Reagents and synthesis of adsorbents

The reagents utilized in this study were of analytical grade (A.R.). The aqueous solutions were employed with deionized water. The Mg/Al layer double hydroxides was synthesised using the co-precipitation method[23]. Starch-stablized layer double hydroxides (S-LDH) were synthesised by the modified co-precipitation method. Firstly, 10mg of starch is dispersed in 1000ml aqueous solution to form starch solution. Secondly, a combined solution of 0.50 mol of $Al(NO_3)_3{\cdot}9H_2O$ and 1.50 mol of $Mg(NO_3)_2{\cdot}6H_2O$ and a combined solution of 0.5 mol/L Na_2CO_3 and 2.00 mol/L NaOH mixed with starch solution slowly accompanied with vigorously stirring to maintain the pH at arount 10. Subsequently, the suspension was aged, separated, dried. At last, the resulting material passed through a 60 mesh screen and collected for later use.

2.2. Characterization methods

The materials surface features were obtained by the Fourier Transform Infrared (FT-IR) spectrums on a Bruker TENSOR27 spectrophotometer within the limit of 400-4,000 cm^{-1}. The materials elements were analyzed by the X-ray powder diffraction pattern (XRD) patterns in Bruker D8 X(Germany). The scanning scope is 5º~80º every 0.02º (2θ) with a step speed of 8°·min^{-1}. The particle size distribution was determined by Zetasizer NANO ZS90(England) with the maximum particle size range of 0.3nm-10μm, concentration range of 0.1 ppm - 40 % w/v and detection angle of 175º, 12.8º.

2.3. Experimental procedure

Adsorption experiments were investigated in lab-scale application. Adsorption isotherms were gained by mixing 0.2g S-LDH with 50 mL of water with fluoride concentration of 10mg/L, 20mg/L, 50mg/L, 80mg/L and 100mg/L and the fluoride concentrations under equilibrium condition were tested after 4 hour's reaction. The kinetics experiment of fluoride adsorption was obtained with the dosage of S-LDH 0.2 g combining with fluoride initial concentration of 10 mg/L in a conical flask with 50 mL of water and the residual fluoride concentration was measured after a different contact time. The whole experiments were done in a thermostat with continuous oscillation at 180 rpm, 20±1 °C. After reaction the adsorbent was separated by filtration.

The adsorption value of fluoride on S-LDH could be calculated as follows[24] :

$$q_e = \frac{(C_0 - C_e)V}{W}, \quad (1)$$

where q_e is the amount of fluoride adsorbed on S-LDHs at equilibrium time; C_0 (mg/L) is the initial fluoride concentration and C_e (mg/L) is the equilibrium fluoride concentration; V is the volume of solution (L); W is the weight of adsorbent (g).

3. Results and Discussion

3.1. Characteristics of LDHs

Representative XRD patterns of the Mg-Al LDH and starch-based LDH adsorbents are displayed in Figure 1. It can be seen that Mg-Al LDH materials displays sharp peaks in (003), (006), (013), showing that the materials are the characteristic reflections of the layer double hydroxides structure (Figure 1a). As for the samples with starch stablized, the characteristics of the original diffraction peak still exist, but the peak value is weakened, the width of the characteristic peak is broadened, indicating that the material has changed (Figure 1b). The XRD patterns after the fluoride adsorption in Figure 1c, the peaks in (003), (006) and (009) becomes wider and the peak strength becomes weaker, which shows that the material crystallinity reduced in after adsorption.

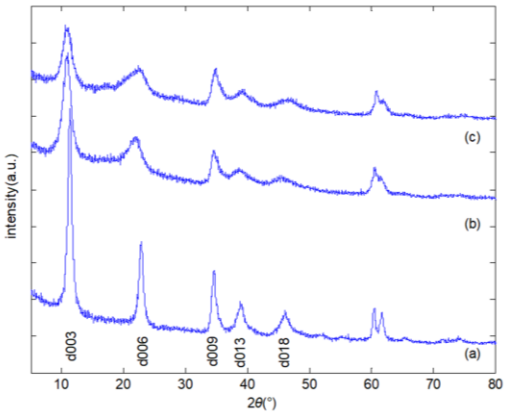

Figure 1. XRD pattern of (a)Mg/ Al LDH, (b)S-LDH, (c)Samples after fluoride removal on S-LDH.

FT-IR study of Mg-Al LDH, S-LDH and S-LDH before and after adsorption were exhibited to detect the presence of characteristic functional groups. As can be seen from the Figure 2a in the FT-IR spectrum, the region between 3400 and 3700 cm^{-1} has broad bands for -OH stretching vibrations of hydroxyl groups[25]. The band at 1653 cm^{-1} is for the adsorbed inter-layer water. The peak at 1372 cm^{-1} is for the vibration of CO_3^{2-} and NO_3^-. The band below 1000 cm^{-1} is for the metal bands. While for the FT-IR spectrum of S-LDH (Figure 2b), the weak band at ~1315 cm^{-1} and ~1030cm^{-1} is assigned to CH_2–O–CH_2[26], indicating that starch and LDHs effectively bonded together. The FT-IR spectra of the S-LDH after fluoride adsorption in Figure 2c, the band at 3503 cm^{-1} was shifted to 3468 cm^{-1}, showing that anions and the hydroxyl groups interacted on adsorbent.

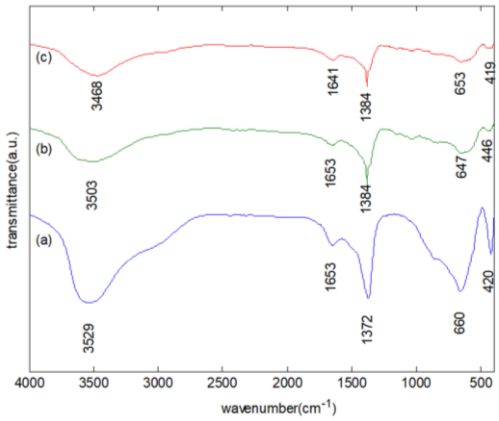

Figure 2. FT-IR pattern of (a)Mg/ Al LDH, (b)S-LDH, (c)Samples after fluoride removal on S-LDH.

The particle size distribution of Mg/Al LDHs and S-LDH is shown in Figure 3. It can be seen that the average diameter of is 1358nm and the particle size distribution is scatted. The average particle size of S-LDH was 421 nm, and the particle size distribution was relatively concentrated, which showed that the particle size distribution of the starch stabilized was more uniform.

Preprints (www.preprints.org) | NOT PEER-REVIEWED | Posted: 15 May 2018 doi:10.20944/preprints201805.0217.v1

Peer-reviewed version available at Water 2018, 10, 745; doi:10.3390/w10060745

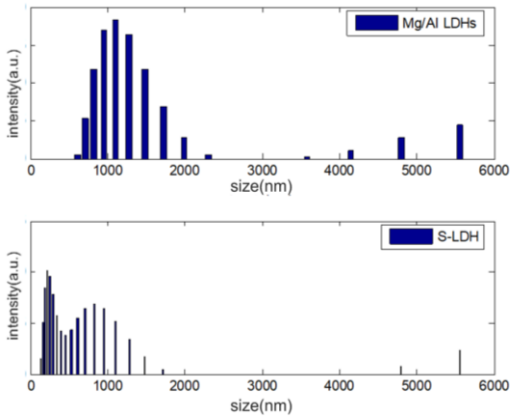

Figure 3. Size distribution of Mg/Al LDHs and S-LDH.

3.2. Adsorption study

3.2.1. Dosage effect of starch content

The dosage effect of starch on fluoride removal is displayed in Figure 4. It can be seen that starch content has obvious effect on fluoride removal. The removal rate increased greatly with the increment of the starch dosage. When the dosage amount of starch is about 10mg, the removal percentage of fluoride reached 98%, which is 3 times higher than the removal rate of the Mg/Al LDH. The first reason is that the starch is anion state under alkaline condition, inhibiting the entry of carbon dioxide and increasing the removal rate of fluoride. The second reason is that the starch promotes the higher dispersion of LDH, thus increasing the surface area of S-LDH and making the adsorption point more abundant.

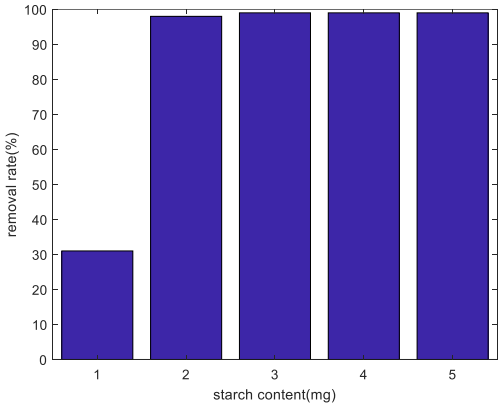

Figure 4. Effect of starch content on fluoride removal.

3.2.2. Adsorption isotherm

The experimental adsorption data of fluoride on S-LDH is determined by the isotherm models of Langmuir and Freundlich. [27] Langmuir isotherm model supports monolayer adsorption, and Freundlich isotherm is related to multi-layer, non-linear adsorption process. The correlation coefficient (R^2) and The root mean square error （(RSME) are compared and evaluated which is the best fit of the two isotherms.

The linearized expression of Langmuir isotherm is:

$$\frac{C_e}{q_e} = \frac{C_e}{q_m} + \frac{1}{K_L q_m}, \quad (2)$$

The linearized expression of Freundlich isotherm is:

$$\ln q_e = \ln K_F + \frac{1}{n} \ln C_e, \quad (3)$$

Preprints (www.preprints.org) | NOT PEER-REVIEWED | Posted: 15 May 2018 doi:10.20944/preprints201805.0217.v1

Peer-reviewed version available at Water 2018, 10, 745; doi:10.3390/w10060745

where q_m is the calculated adsorption amount (mg/g); K_L is the Langmuir constant (L/mg). K_F is the Freundlich constant; 1/n is the heterogeneity factor.

RMSE was calculated for evaluating the straight line fit and the equations is as follows[28]:

$$RMSE = [\sum (q_t - q_t^*)^2 / (n-m)]^{0.5}, \quad (4)$$

Where q_t is the adsorbed(mg/g) at time t gained from the lab experiments, and q_t* is the fluoride capacity adsorbed(mg/g) forecasted by the two models. the samples number is expressed by the n value and fitted parameters number is expressed by the m value.

Figure 5 and Table 1 showed the results of isotherm curves fitting with Freundlich and Langmuir equations. The results showed that the Langmuir isotherm model had higher R^2 and lower RMSE value, which indicate that the reaction process might be monolayer adsorption with chemisorption on the adsorbent surface. It can be seen that the maximum adsorption capacity is 21.72 mg/g, which is 3 times higher than the value of previous investigated for Mg/Al LDH. The value of K_L was greater than zero, indicating that adsorption system was favorable.

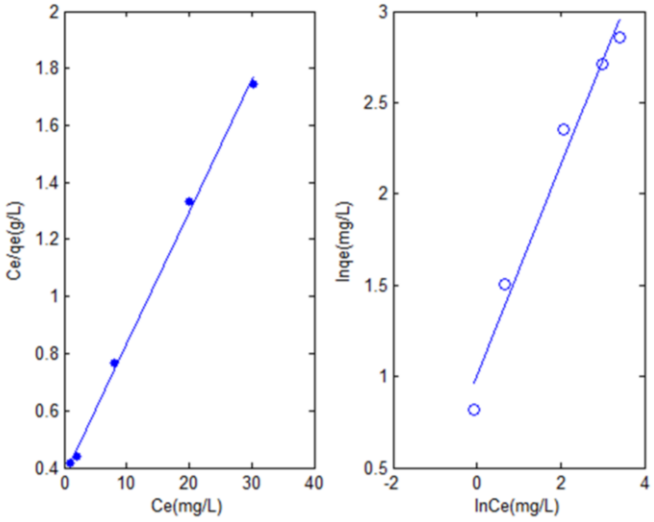

Figure 5. Curve fit of Langmuir and Freundlich isotherm.

Table 1. Isotherm adsorption models of fluoride onto S-LDH.

Langmuir isotherm				Freundlich isotherm			
K_L	q_m(mg/g)	R^2	RMSE	K_F	n	R^2	RMSE
0.123	21.72	0.9987	0.0102	2.719	1.7393	0.9884	0.0804

3.2.3. Adsorption kinetic studies

The adsorption kinetics can identify the process of the adsorption efficiency and help to verify the fluoride adsorption mechanism. The adsorption rate and fluoride uptake kinetics on S-LDHs were studied based on two reaction based models (pseudo first and pseudo second) and diffusion based model (intraparticle diffusion model). The pseudo-first order model assumes the reaction is reversible, the pseudo-second order model regards chemisorption as the rate limiting step. The intraparticle diffusion assumes that the plots pass through origin. The models can be expressed as follows[29]:

pseudo-first order model[30] $$\ln(q_e - q_t) = \ln(q_e) - k_1 t, \quad (5)$$

pseudo-second order model[31] $$\frac{t}{q_t} = \frac{1}{k_2 q_e^2} + \frac{t}{q_e} \quad (6)$$

intraparticle diffusion model[32] $q_t = K_F t^{1/2} + C$ (7)

The common parameters, k_1 represents the rate constant of adsorption (min^{-1}) obtained from the plot of $\ln(q_e-q_t)$ against t. k_2 means the pseudo-second rate constant(g/(mg·min)) obtained from the linear plot of t/q_t against t. K_F is the intraparticle diffusion rate constant ($mg/(g\cdot min^{0.5})$).

The results of fitting kinetics models were summarized in Figure 6 and Table 2. pseudo-second order kinetic was proved to be fitted with the experiment data by the high R^2 (>0.99) and low RMSE, which implied chemisorption. The values of k_2 was low, indicating that the adsorption process rates were fast.

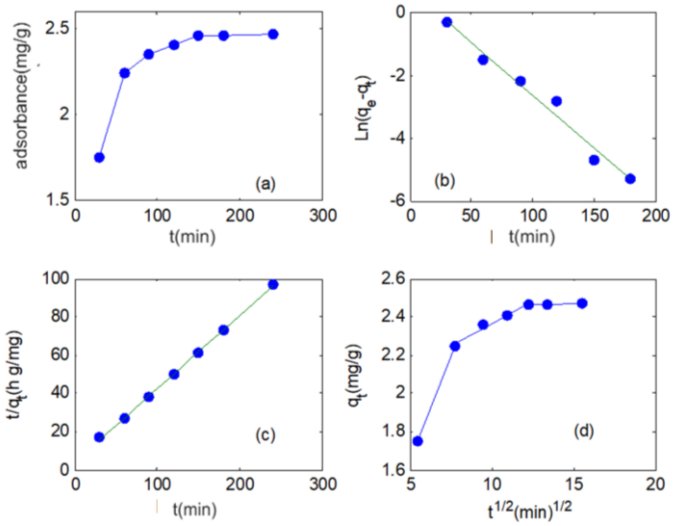

Figure 6. Kinetics of fluoride adsorption on the S-LDH from (a) experiment, models by (b) pseudo first, (c) pseudo second, and (d) intraparticle diffusion

Table 2. Adsorption kinetic models for fluoride removal on S-LDH and the calculated constants

Kinetic Models	parameter			
Pseudo-first-order	k_1 (min^{-1})	q_e(mg/g)	R^2	RMSE
	0.0771	2.036	0.9872	0.2401
Pseudo-second-order	k_2 (g/(mg·min))	q_e(mg/g)	R^2	RMSE
	0.1467	2.6107	0.9995	0.1194
intraparticle diffusion	k_F($mg/(g\cdot min^{0.5})$)	R^2	RMSE	
	2.4289	0.8471	0.7321	

3.2.4. Adsorption thermodynamics studies

Variation of temperature can be used to analysis the thermodynamic properties of LDHs–fluoride interaction. In this study, temperature was controlled in a range of 20~50℃.. ΔG^0, ΔS^0 and ΔH^0 were calculated by Van't Hoff equation:

$$\triangle G^0=-RT\ln b, \quad (8)$$

Error! Reference source not found. (9)

$$\ln b = \frac{\Delta S^0}{R} - \frac{\Delta H^0}{RT}, \quad (10)$$

where, R is the universal gas constant (8.314J·mol^{-1} K^{-1}), b is adsorption isothermy constant, ΔG^0 is the change in free energy, ΔH^0 is the standard enthalpy and ΔS^0 is the standard entropy, T is the temperature (K),. Here, b value can be calculated from the Langmuir constant $K_L \cdot Q_m$. ΔH^0 and ΔS^0 parameters can be obtained, respectively, from the slope and intercept of plot of lnb vs. 1/T. The results are shown in Table 3. It can be seen that the values of ΔG^0 is negative, indicating sorption process is the spontaneous nature. As the temperature rises, the reaction becomes relatively easy. The positive value of ΔH^0 confirms the sorption process is endothermic . The positive value of ΔS^0

Preprints (www.preprints.org) | NOT PEER-REVIEWED | Posted: 15 May 2018 doi:10.20944/preprints201805.0217.v1

Peer-reviewed version available at Water 2018, 10, 745; doi:10.3390/w10060745

indicates that the reaction is spontaneous, and the solid-liquid interface is random at the time of adsorption.

Table 3. The value of thermodynamic parameter for the adsorption of fluoride by the S-LDH.

Temperature (℃)	b	Thermodynamic parameter		
		△G⁰ (KJ/mol)	△H⁰ (KJ/mol)	△S⁰(J/(mol·K))
20	9.73	-12.44	35.63	0.0806
30	4.25	-10.78		
40	2.67	-9.93		
50	2.55	-10.12		

Arrhenius equation represent the variance between temperature and activation energy of adsorption. Activation energy calculation can be obtained using the formula 15.

$$k=Ae^{-Ea/RT}, \quad (11)$$

where, k is pseudo second-order reaction rate constant, (g/(mg·min)), Ea is activation energy, (kJ/mol). The calculated activation energy is 38.83kJ/mol, greater than 20KJ/mol, indicating the reaction is corresponded to the slow defluorination stage, controlled by the chemical reaction of fluoride ion and S-LDHs.

3.3. mechanism analysis

pH value is an important parameter for reflecting adsorption property. In this paper, The isoelectric point (pH_{PZC}) and variance of pH value was used to analyzed proposed adsorption mechanism. pH_{PZC} plays an important role on the surface properties of the material, determining the degree of difficulty of adsorption. The pH_{PZC} of adsorbent can be determined by salt supplement method[33]. As shown in Figure 7, pH_{PZC} of the S-LDH adsorbents is 9.22. The results of the variance of initial pH value to the fluoride adsorption on S-LDH at 20°C were also analyzed. It can be seen that with the initial pH value in the solution varying from 3.0 to 9.0, the adsorption capacity of fluoride onto the material kept stable, while when pH value was higher than 9.0, the adsorption capacity of fluoride decreased gradually, but still kept a comparably high level, indicating that a wide range of intial pH value has little effect on the removal ability of fluoride. When pH value is less than pH_{PZC}, the charge surface is positively charged, while when pH value is higher than pH_{PZC}, the charge surface is negatively charged. So the possible reason is as follows: Under acidic conditions, the protonation makes the surface of the adsorbent positively charged, fluoride ions are more easily adsorbed onto S-LDH. Under alkaline conditions, OH^- concentration in solution increases, and competes with fluoride ion, indicating that fluoride ions could not effectively enter the layer of S-LDH. The reason why the removal rate of fluoride ions is still high under alkaline conditions is that the surface of the starch is positively charged and fluoride ions are efficiently adsorbed. In summary, according to adsorption experiments and characterization analysis, fluoride ion adsorption by S-LDH is presumed mainly by the interaction of LDH and surface adsorption of S-LDH.

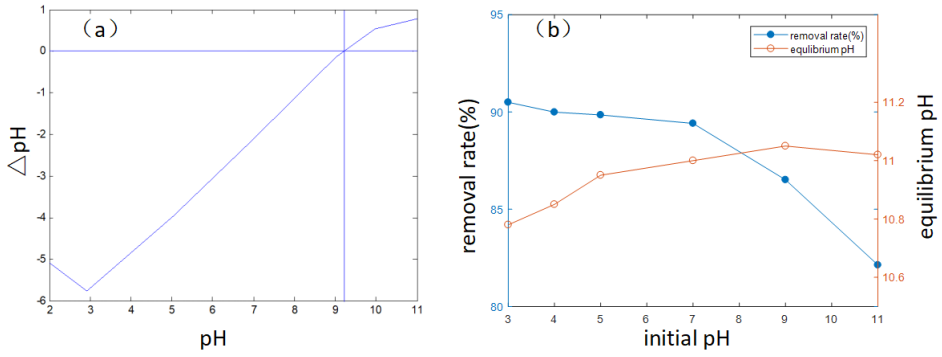

Figure 7. pHpzc of S-LDH and effect of initial pH on the fluoride removal

4. Conclusions

In this work, starch stablized Mg-Al-LDHs were utilized as adsorbents and the property of Mg/Al LDH and S-LDH were compared. The fluoride adsorption capacity of the S-LDH was 3 times higher than that of the Mg/Al LDH. The particle size distribution of the S-LDH is more uniform than that of LDH. Langmuir adsorption isotherm model and pseudo-second-order kinetic model fitted well with the experimental data. In thermodynamic parameters, the enthalpy (ΔH^0) value was 35.63 kJ mol^{-1} and the entropy (ΔS^0) value was 0.0806 kJ $mol^{-1}K^{-1}$. The negative values of $\triangle G^0$ indicate the spontaneous nature of adsorption. The change in a wide range of intial pH value has little effect on the removal ability of fluoride. The mechanism for fluoride removal on S-LDH included surface adsorption and interaction ion exchange. Further investigations could focus on reuse of the material and dynamics monitor with real water.

Acknowledgments: The authors are grateful for the financial support from Shanxi Provincia Natural Science Foundation, China (Grant No. 201601D102037).

Conflicts of Interest: There are no conflicts to declare.

References

1. Chen P, Wang T, Xiao Y, Tian E, Wang W, Zhao Y, Tian L, Jiang H, Luo X: **Efficient fluoride removal from aqueous solution by synthetic Fe-Mg-La tri-metal nanocomposite and the analysis of its adsorption mechanism.** *J Alloy Compd* 2018, **738:**118-129.
2. Theiss FL, Couperthwaite SJ, Ayoko GA, Frost RL: **A review of the removal of anions and oxyanions of the halogen elements from aqueous solution by layered double hydroxides.** *J Colloid Interf Sci* 2014, **417:**356-368.
3. Sakhare N, Lunge S, Rayalu S, Bakardjiva S, Subrt J, Devotta S, Labhsetwar N: **Defluoridation of water using calcium aluminate material.** *Chem Eng J* 2012, **203:**406-414.
4. Zhu X, Yang C, Yan X: **Metal-organic framework-801 for efficient removal of fluoride from water.** *Micropor Mesopor Mat* 2018, **259:**163-170.
5. Gao C, Yu X, Luo T, Jia Y, Sun B, Liu J, Huang X: **Millimeter-sized Mg–Al-LDH nanoflake impregnated magnetic alginate beads (LDH-n-MABs): a novel bio-based sorbent for the removal of fluoride in water.** *J Mater Chem A* 2014, **2:**2119-2128.
6. He J, Chen JP: **A zirconium-based nanoparticle: Essential factors for sustainable application in treatment of fluoride containing water.** *J Colloid Interf Sci* 2014, **416:**227-234.
7. WHO World Health Organization: **Guidelines for Drinking-Water Quality, fourth ed.** (World Health Organization ed. pp. 371. Geneva; 2011:371.
8. Grzegorzek M, Majewska-Nowak K: **The influence of organic matter on fluoride removal efficiency during the electrodialysis process.** *Desalin Water Treat* 2017, **69:**153-162.
9. Yu Z, Xu C, Yuan K, Gan X, Feng C, Wang X, Zhu L, Zhang G, Xu D: **Characterization and adsorption mechanism of ZrO_2 mesoporous fibers for health-hazardous fluoride removal.** *J Hazard Mater* 2018, **346:**82-92.
10. Jiang H, Zhang W, Chen P, He Q, Li M, Tian L, Tu Z, Xu Y: **One Pot Method to Synthesize a Novel La–Zr Composite with Exceptionally High Fluoride Removal Performance.** *J Inorg Organomet P* 2016, **26:**285-293.
11. Kang D, Yu X, Ge M: **Morphology-dependent properties and adsorption performance of CeO2 for fluoride removal.** *Chem Eng J* 2017, **330:**36-43.
12. Wan D, Liu Y, Xiao S, Chen J, Zhang J: **Uptake fluoride from water by caclined Mg-Al-CO3 hydrotalcite: Mg/Al ratio effect on its structure, electrical affinity and adsorptive property.** *Colloids and Surfaces A: Physicochemical and Engineering Aspects* 2015, **469:**307-314.

13. Liu S, Ye X, He K, Chen Y, Hu Y: **Simultaneous removal of Ni(II) and fluoride from a real flue gas desulfurization wastewater by electrocoagulation using Fe/C/Al electrode.** *J Water Reuse Desal* 2017, **7:**288-297.

14. Markovski J, Garcia J, Hristovski KD, Westerhoff P: **Nano-enabling of strong-base ion-exchange media via a room-temperature aluminum (hydr)oxide synthesis method to simultaneously remove nitrate and fluoride.** *Sci Total Environ* 2017, **599-600:**1848-1855.

15. Agbaje TA, Al-Gharabli S, Mavukkandy MO, Kujawa J, Arafat HA: **PVDF/magnetite blend membranes for enhanced flux and salt rejection in membrane distillation.** *Desalination* 2018, **436:**69-80.

16. Theiss FL, Couperthwaite SJ, Ayoko GA, Frost RL: **A review of the removal of anions and oxyanions of the halogen elements from aqueous solution by layered double hydroxides.** *J Colloid Interf Sci* 2014, **417:**356-368.

17. Gao C, Yu X, Luo T, Jia Y, Sun B, Liu J, Huang X: **Millimeter-sized Mg–Al-LDH nanoflake impregnated magnetic alginate beads (LDH-n-MABs): a novel bio-based sorbent for the removal of fluoride in water.** *J Mater Chem A* 2014, **2:**2119-2128.

18. Hu P, Zhang Y, Lv F, Tong W, Xin H, Meng Z, Wang X, Chu PK: **Preparation of layered double hydroxides using boron mud and red mud industrial wastes and adsorption mechanism to phosphate.** *Water Environ J* 2017, **31:**145-157.

19. Shan R, Yan L, Yang K, Hao Y, Du B: **Adsorption of Cd(II) by Mg–Al–CO3- and magnetic Fe3O4/Mg–Al–CO3-layered double hydroxides: Kinetic, isothermal, thermodynamic and mechanistic studies.** *J Hazard Mater* 2015, **299:**42-49.

20. Moriyama S, Sasaki K, Hirajima T: **Effect of calcination temperature on Mg-Al bimetallic oxides as sorbents for the removal of F- in aqueous solutions.** *Chemosphere* 2014, **95:**597-603.

21. Xu L, Chen G, Peng C, Qiao H, Ke F, Hou R, Li D, Cai H, Wan X: **Adsorptive removal of fluoride from drinking water using porous starch loaded with common metal ions.** *Carbohyd Polym* 2017, **160:**82-89.

22. Liang Q, Zhao D: **Immobilization of arsenate in a sandy loam soil using starch-stabilized magnetite nanoparticles.** *J Hazard Mater* 2014, **271:**16-23.

23. Lv L: **Defluoridation of drinking water by calcined MgAl-CO3 layered double hydroxides.** *Desalination* 2007, **208:**125-133.

24. Swain SK, Patnaik T, Singh VK, Jha U, Patel RK, Dey RK: **Kinetics, equilibrium and thermodynamic aspects of removal of fluoride from drinking water using meso-structured zirconium phosphate.** *Chem Eng J* 2011, **171:**1218-1226.

25. Sun Z, Park J, Kim D, Shin C, Zhang W, Wang R, Rao P: **Synthesis and Adsorption Properties of Ca-Al Layered Double Hydroxides for the Removal of Aqueous Fluoride.** *Water Air Soil Poll* 2017, **228**.

26. Mandal S, Mayadevi S: **Cellulose supported layered double hydroxides for the adsorption of fluoride from aqueous solution.** *Chemosphere* 2008, **72:**995-998.

27. Zhao W, Chen Y, Zhang W: **Rapid and convenient removal of fluoride by magnetic magnesium-aluminum-lanthanum composite: Synthesis, performance and mechanism.** *Asia-Pac J Chem Eng* 2017, **12:**640-650.

28. Halajnia A, Oustan S, Najafi N, Khataee AR, Lakzian A: **Adsorption-desorption characteristics of nitrate, phosphate and sulfate on Mg-Al layered double hydroxide.** *Appl Clay Sci* 2013, **80-81:**305-312.

29. Vazquez Mejia G, Solache-Rios M, Martinez-Miranda V: **Removal of fluoride and arsenate ions from aqueous solutions and natural water by modified natural materials.** *Desalin Water Treat* 2017, **85:**271-281.

30. El-Said GF, El-Sadaawy MM, Aly-Eldeen MA: **Adsorption isotherms and kinetic studies for the defluoridation from aqueous solution using eco-friendly raw marine green algae, Ulva lactuca.** *Environ Monit Assess* 2018, **190:**1-15.

31. Türker OC, Baran T: **A combination method based on chitosan adsorption and duckweed (Lemna gibba L.) phytoremediation for boron (B) removal from drinking water.** *Int J Phytoremediat* 2018, **20:**175.

32. Ren G, Wang X, Huang P, Zhong B, Zhang Z, Yang L, Yang X: **Chromium (VI) adsorption from wastewater using porous magnetite nanoparticles prepared from titanium residue by a novel solid-phase reduction method.** *Sci Total Environ* 2017, **607-608:**900-910.

33. Dayananda D, Sarva VR, Prasad SV, Arunachalam J, Ghosh NN: **Preparation of CaO loaded mesoporous Al_2O_3: Efficient adsorbent for fluoride removal from water.** *Chem Eng J* 2014, **248:**430-439.